

## Plasma dynamics from laser ablated solid lithium

DEBARATI BHATTACHARYA

Institute for Plasma Research, Bhat, Gandhinagar 382 428, India

Present address: Nuclear Science Centre, Aruna Asaf Ali Marg, Post Box No. 10502,  
New Delhi 110 067, India

**Abstract.** Emission plasma plume generated by pulsed laser ablation of a lithium solid target by a ruby laser (694 nm, 20 ns, 3 J) was subjected to optical emission spectroscopy: time and space resolved optical emission was characterised as a function of distance from the target surface. Propagation of the plume was studied through ambient background of argon gas. Spectroscopic observations can, in general, be used to analyse plume structure with respect to an appropriate theoretical plasma model. The plume expansion dynamics in this case could be explained through a shock wave propagation model wherein, the experimental observations made were seen to fit well with the theoretical predictions. Spectral information derived from measurement of peak intensity and line width determined the parameters, electron temperature ( $T_e$ ) and electron number density ( $n_e$ ), typically used to characterise laser produced plasma plume emission. These measurements were also used to validate the assumptions underlying the local thermodynamic equilibrium (LTE) model, invoked for the high density laser plasma under study. Some interesting results pertaining to the analysis of plume structure and spatio-temporal behaviour of  $T_e$  and  $n_e$  along the plume length will be presented and discussed.

**Keywords.** Laser ablation; plasma dynamics; optical emission spectroscopy.

**PACS Nos** 32.70.-n; 42.62.-b; 52.25.-b; 52.70.-m

### 1. Introduction

Pulsed laser ablation of a solid sample generates a dense plasma emission in the shape of a ‘plume’, comprising atomic, ionic and neutral species of the target element, along with electrons and photons. Analysis of spectroscopic information gleaned from this laser produced plasma (LPP) emission [1] has gained importance due to various applications linked to properties of the emissive plasma. Study of LPP is of utmost interest especially in the fields of thin film growth, laser diagnostics, elemental trace analysis wherein it finds wide application [2]. Coupling of laser energy to materials in LPPs finds applications in machining, welding, hole boring and in soft X-ray laser experiments wherein temporal evolution of ablation plasma plays an important role [3]. Among the several diagnostic techniques generally used to probe the LPP emission for its characteristic properties, *optical emission spectroscopy* appears to be a popular choice owing to its non-intrusive and sensitive character.

The present work deals with ruby laser ablation of a solid lithium target and characterisation of the ensuing plasma plume. Spatially resolved real time optical emission

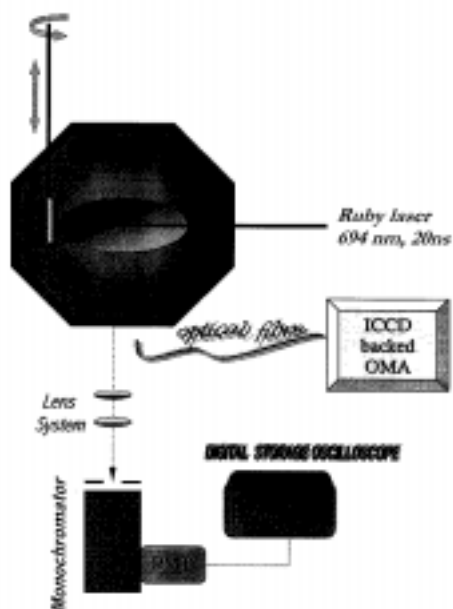


**Figure 1.** Schematic of experimental set-up for laser ablation of solid lithium target.

spectroscopy has been used in order to investigate the influence of gas pressure on the plume expansion process. For this purpose, evolution of the emission intensity of excited species  $\text{Li}^* \text{I}$  (670.8 nm) with distance from the target surface ( $r$ : 2 to 10 mm), through argon background gas at different pressures ranging from  $10^{-5}$  mbar to 1 mbar has been measured.

## 2. Experimental setup

The experimental system (vacuum chamber) with associated equipments set up for the study of laser ablated Li plasma dynamics is shown in figure 1. A ruby laser (694.3 nm, 20 ns, 3 J) was focused normal to the target, capable of two dimensional motion. The target used was in the form of a 6 cm long Li rod ( $\sim 1.27$  cm diameter). The laser was focused to an energy density of  $\sim 18 \text{ J/cm}^2$ . The plasma emission was viewed normal to its direction of propagation and scanned (for wavelengths corresponding to Li (I): 670.8 nm, 610.4 nm, 497.2 nm, 460.3 nm) along the plume axis by optical emission spectroscopy, in order to investigate propagation through ambient background of argon gas. The experiment was performed in vacuum ( $10^{-6}$  mbar) and in an argon gas environment ( $10^{-5}$  to 1 mbar).

The light emitted was imaged onto the entrance slit of a 0.35 m Jobin-Yvon monochromator ( $\Delta\lambda = 1.25 \text{ nm}$ ) by means of a two lens system with unity magnification, giving a spatial resolution of  $250 \mu\text{m}$  along the target normal. The monochromator along with the lens system was moved on a X-Y translator system for well controlled scan of the plume along its expansion axis. A photomultiplier tube (2 ns rise time) was connected to a fast

digital storage oscilloscope for intensity measurements. Time and space resolved optical emission from the plasma was characterised as a function of distance from target surface and ambient argon gas pressure. The evolution of time delay and velocity of excited Li (I) species at 670.8 nm were determined. Li emission intensity measurements were made in the presence of varying gas pressures at intervals of 2 mm upto 10 mm from the target.

In order to obtain temporally resolved optical spectra of laser induced ablation plasma at various points along the plume, light from emission was also collected by a 400  $\mu\text{m}$  optical fibre. The optical system was precisely aligned with He–Ne laser beam. Spectra were recorded around the particular wavelength and output signal coupled to an image-intensified charge coupled device (ICCD) camera backed optical multichannel analyser (Princeton Instruments) covering nearly 280 Å per frame with one-to-one imaging of the emission. The multichannel analyser plate of the ICCD was gated for as less as 4 ns using a fast programmable pulsar (Princeton Instruments PG200) which was synchronised with a photo diode signal. Wavelength correction was performed using a standard tungsten filament lamp. Gates were moved relative to laser output, therefore, temporal evolution of rapidly varying ablation plasma could be obtained. Spectra were viewed on a cathode ray oscilloscope and the images were stored and processed by a computer connected via GPIB interface.

### 3. Results and discussion

Emission plasma plume generated by ablation of a lithium solid target by a pulsed ruby laser, was subjected to scanning by optical emission spectroscopy in order to investigate behaviour of excited states of ablated species and propagation of the plume through ambient background of argon gas. Time and space resolved optical emission from the plasma was characterised as a function of distance from target surface ( $r$ : 0 to 10 mm) and ambient argon gas pressure (in the range:  $10^{-5}$  to 1 mbar).

#### 3.1 Determination of $T_e$ and $n_e$ : Application of local thermodynamic equilibrium model

Spectroscopic observations which are made can in general be used to analyse plume structure with respect to an appropriate theoretical plasma model. For a high density laser plasma one invokes the concept of local thermodynamic equilibrium (LTE) as a model to explain the atomic collision processes [4]. The experimental results when fitted to the proposed model, will validate the assumptions underlying the model [5]. An applicability criterion of LTE has been defined [6] with the consideration that the collisional rates exceed the radiative rates. Thus the plasma, if it is to be in LTE, must validate the condition,  $n_e \geq 1.6 \times 10^{12} T_e^{0.5} (E^*)^3$ , where,  $T_e$  is in K and  $E^*$ , the largest energy gap for which the condition holds, is in eV. In accordance with LTE,  $T_e$  and  $n_e$  were obtained through spectroscopic line intensity measurements and the variation of these parameters along the plume length provided ample information to define the plume behaviour.

Spectral lines observed in the Li plasma were collisionally broadened by Stark effect. The effect of Doppler broadening was ignored due to the high expansion velocities of Li (I) obtained in the plasma. Theoretical profile was varied until best possible fit with measured lineshape was achieved [7]. In this case, the emission lines could be approximated by a Lorentzian profile. Figure 2 shows a Lorentzian curve fitted to the Stark broadened profile

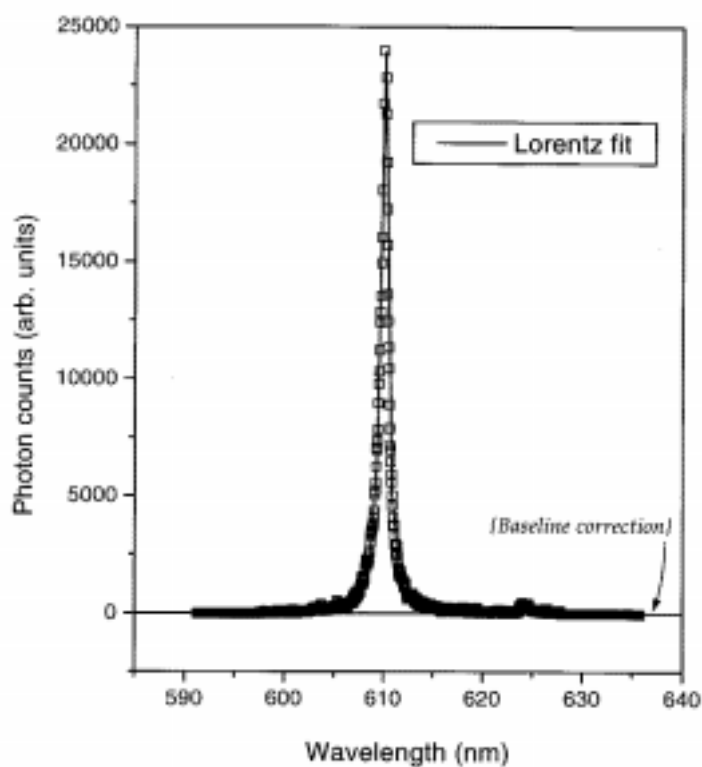


**Figure 2.** A typical Stark broadened profile of Li (I) obtained for 610.4 nm with ruby laser irradiation, at 4 mm from the target in 1 mbar argon (gate width:150 ns, gate delay: 800 ns). A Lorentzian profile (solid line in figure) appears to fit the experimental data very well.

of Li (I) obtained at 610.4 nm at a distance of 4 mm from the target. Stark broadening from electron impact with thermal atoms is a dominant effect in dense plasmas and is widely used for electron number density measurements [5,8,9]. Correction of line profiles for underlying continuum was carried out to determine, the full widths at half maxima (FWHM) of the lines, used in the density calculations. Collisional excitations of high energy electrons cause higher population densities of excited states of Li atoms.

FWHM  $\Delta\lambda_{(1/2)}$  of the spectral lines were used for the estimation of electron number density (in  $\text{cm}^{-3}$ ) through the relation [10],  $\Delta\lambda_{(1/2)} = 2W(n_e/10^{16}) \text{ \AA}$ , where  $W$  is the electron impact parameter and a weak function of temperature. This is approximated from the expression given by Griem [5]; in the present case, contribution from the ion broadening factor was neglected in the wake of significant predomination of electron impact in causing Stark broadening. Electron temperature measurements were determined from the intensity ratio of the observed spectral lines and by using spectral parameters given in table 1.

**Table 1.** Parameters related to the 4 wavelengths used in the analysis of plasma emission scanned.

Wavelength (Å)	Upper energy level $E_2$ (eV)	Statistical weight $g_2 = 2j + 1$	Transition probability $A_{21}$ ( $s^{-1}$ )
6707.84	1.85	6	$3.72 \times 10^7$
6103.64	3.88	10	$7.16 \times 10^7$
4971.99	4.34	2	$1.01 \times 10^7$
4602.90	4.54	10	$2.3 \times 10^7$

### 3.2 Shock wave model: Evolution of time delay and velocity; $r$ - $t$ dependence

To the best of our knowledge, the dynamics of Li bulk ablation process has not been investigated so far but on comparison of our results with laser ablation of other materials like superconducting compounds [11], Al [12] and graphite [13], we observe some common features like increase of delay, pulse width and peak intensity with increase in pressure. Figure 3(a) gives the temporal dependence of  $Li^* I$  (670.8 nm) transient emission intensity maximum at 2 mm in different gas pressures. The time delay between the emission intensity maximum and the laser pulse with distance  $r$  is plotted in figure 3(b) at different pressures. Beyond 1 mm, where the continuum radiation from dense plasma is negligible, the delay recorded in vacuum ( $10^{-6}$  mbar) shows a linear dependence on  $r$ . The most probable velocity estimated from the slope of this linear relation is  $1.9 \times 10^6$  cm/s. The observation that the time delay with respect to the laser pulse varies linearly with distance, suggests a free expansion of the plume in vacuum ( $10^{-6}$  mbar). The presence of background gas produces a nonlinear dependence of the delay on the distance ( $r > 6$  mm) and on pressure ( $> 10^{-2}$  mbar). The velocities calculated from the time-of-flight measurements at  $10^{-6}$ ,  $10^{-2}$  and 1 mbar, are plotted in figure 4. It was observed that beyond 6 mm from the target and for pressures greater than  $10^{-2}$  mbar, velocity of excited species slowed down, a trend which was reflected in the nonlinear dependence of distance ( $r$ ) on time delay ( $t$ ) in this region. Within duration of laser pulse, there occurs laser-solid interaction [14] leading to evaporation and further interaction of laser with evaporants constitutes isothermal plasma expansion. After termination of the laser pulse, adiabatic expansion of the plasma takes place. The range of distance considered here lies in an adiabatic expansion regime where the thermal energy is rapidly converted into kinetic energy and the plasma attains extremely high expansion velocity.

For a more quantitative understanding of the expansion dynamics in this case, we have attempted to fit our results to the shock wave model [11,15] which is one of the most widely used among various existing theoretical models. When material expands into background gas, a shock wave is generated at the expansion front, which consequently leads to rise in temperature at the front [16]. Due to excitation in the plume, part of the energy is transferred to excitation energy such that rate of temperature at the front reduces in order to balance plume heat content, i.e. less energy goes to thermal motion. To maintain conservation of energy and momentum, velocity rises; but this effect is not dominant away from the source since temperature falls. According to this model, the expansion motion can be described by an ideal blast wave,  $r = (E/p)^{1/5} t^{2/5} - r_0$  where  $E$  is a constant proportional to laser energy density,  $p$  is the background gas pressure,  $t$  is the time at which the maximum of transient emission with respect to laser pulse is observed, and  $r_0$  is a constant

to account for the fact that a certain time elapses before the emission occurs at  $r = 0$ . For our experimental results, the best fits for the delay corresponding to maximum intensity, calculated using shock wave model for  $\text{Li}^* \text{I}$  at  $10^{-2}$ ,  $10^{-1}$  and 1 mbar, as a function of distance are plotted in figure 5. It is seen that the fitted curves agree very well with the experimental results. Figure 6 is a log-log plot representation based on the data in the previous figure. A linear relationship between  $\log r$  and  $\log t$  is observed, with a slope of 0.4, which means that  $r$  is proportional to the 0.4 power of time, in good agreement with the exponent in the relation governing motion of shock wave front structure through the plasma.

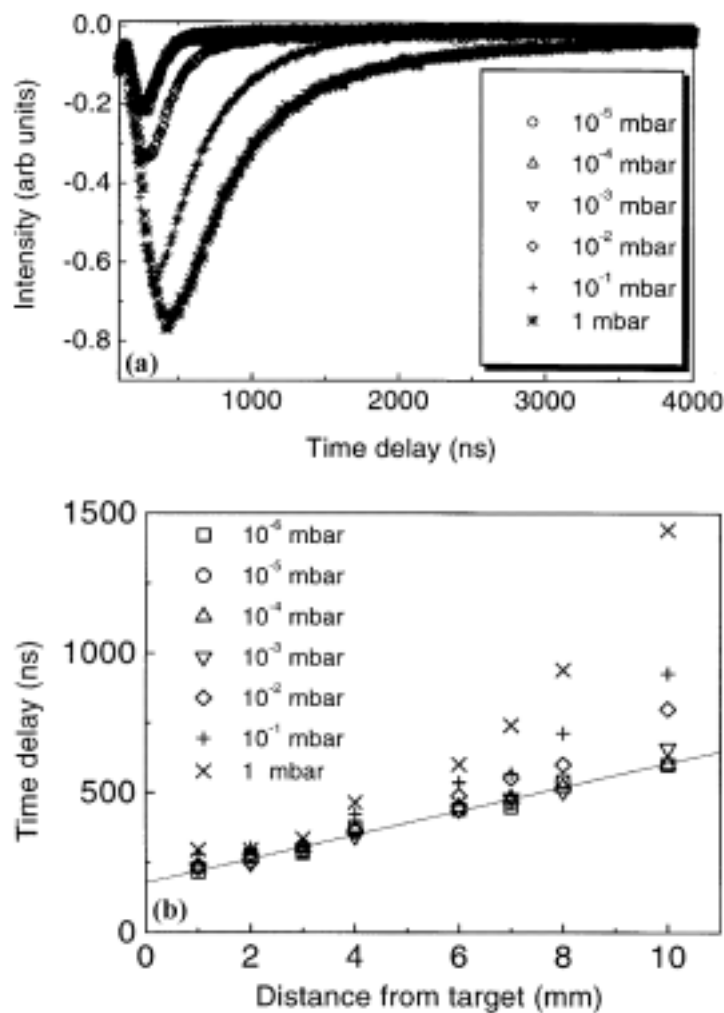


**Figure 3.** (a) Spectral intensity at 2 mm distance from target for different argon gas pressures. (b) Time delay ( $t$ ) dependence on distance from target ( $r$ ) in presence of different argon gas pressures. Delay times indicated are relative to peak of ruby laser pulse.

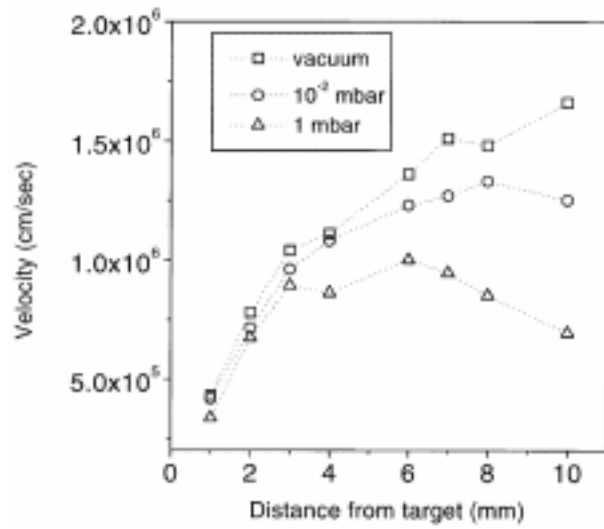


**Figure 4.** Spatial dependence of velocity of plume species in laser produced Li plasma.

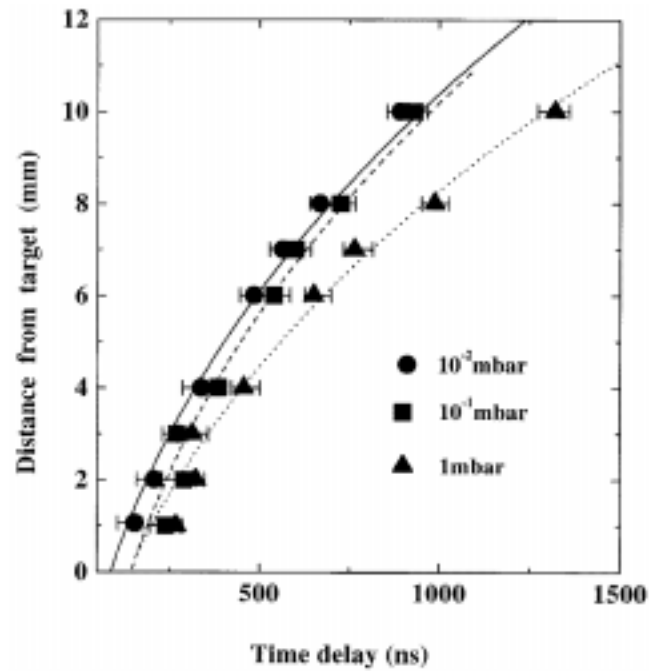


**Figure 5.** Expansion dynamics of laser ablated bulk Li plasma. Curves fitted according to shock wave model ( $r = a t^{0.4} - r_0$ ).

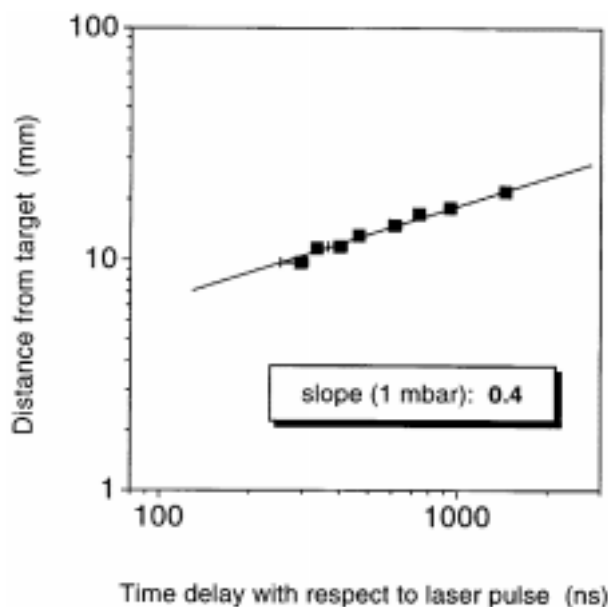


**Figure 6.** Relation between ( $r$ ) distance from target (plume length) and ( $t$ ) transient time delay in a log-log plot.

### 3.3 Variation of $T_e$ and $n_e$ in the plasma plume

Temporal dependence of  $T_e$  followed a  $t^{-1}$  variation regardless of ambient gas pressure, as seen in figure 7, indicating a departure from the theoretical adiabatic expansion model [17]. In this case, the plasma, which is highly collisional to begin with, does not fully recombine. It tends towards a collisionless state with degree of ionisation being frozen. In vacuum,  $n_e$  showed a spatial dependence of  $r^{-1}$ , depicted in figure 8, and a temporal variation of  $t^{-2}$ , seen in figure 9, suggesting linear expansion of plasma in agreement with that observed by others [10,18]. In vacuum, there exists poor coupling between electrons and heavy particles, so any excess energy that the electrons acquire in 3-body recombination cannot be transferred to heavy species. This causes deviation from kinetic equilibrium [19]. An increase in ambient gas pressure caused greater confinement of the plasma by the surrounding gas. The effect of ambient gas was to cool the thermal electrons by enhanced elastic and inelastic collisions, resulting in improved efficiency of atomic collision processes like electron impact and consequently leading to plasma confinement and thereby recombination.

### 4. Further work in progress

Atomic collision processes and excitation mechanisms thereof occurring in the laser produced plasma plume from Li, are being studied in greater detail through experiments conducted with variation in laser irradiance. These are to be reported shortly in a forthcoming paper.



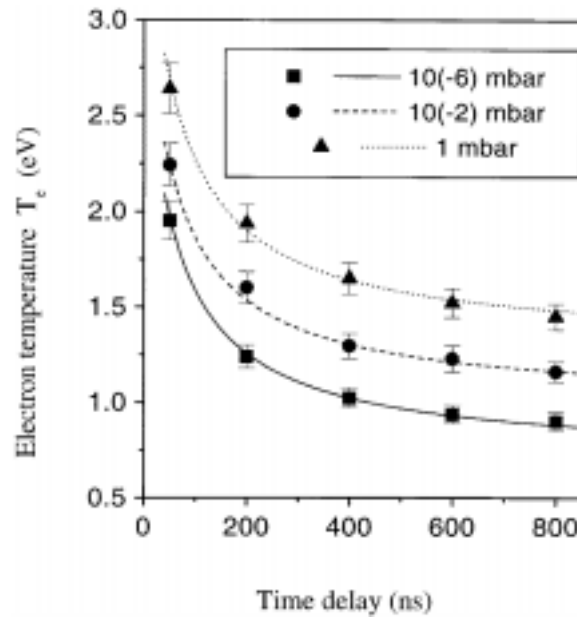


**Figure 7.** Electron temperature change with time delay:  $t^{-1}$  variation. At different pressures and 4 mm distance from the target.

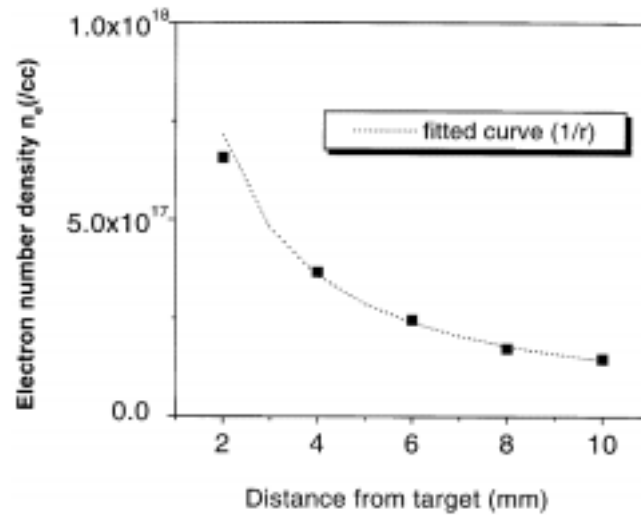


**Figure 8.** Electron density variation with distance from target. Spatial dependence of electron density appears to follow a  $1/r$  relation in  $10^{-6}$  mbar pressure.

Further, it was of interest to compare dynamics of laser produced plasma from LiF-C coated plate (used in laser-blow-off studies to probe edge plasma properties in tokamaks), with that generated from Li solid target ablation. The dynamics of emission from

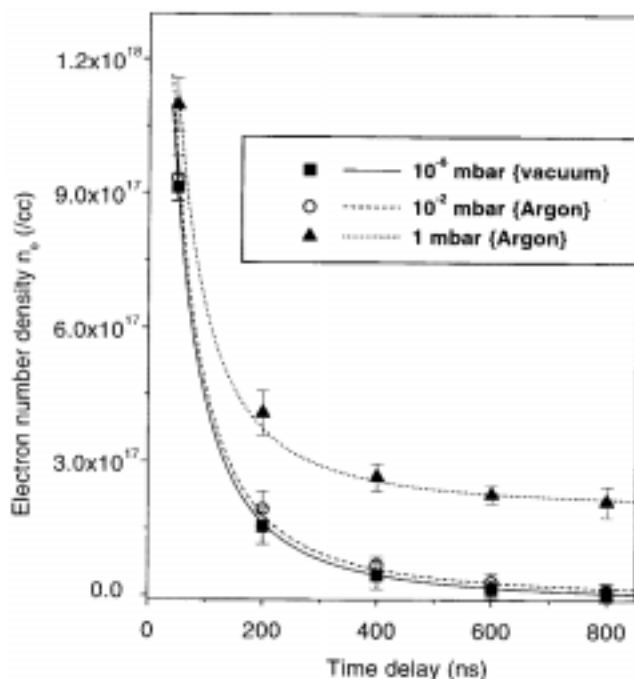


**Figure 9.** Electron number density change with time delay ( $t^{-2}$  variation). At various ambient pressures and 6 mm distance from the target.

the former are not completely understood. The results in case of LPP emission were compared with the laser-blow-off dynamics obtained with the same experimental parameters. It was observed that the dynamics of laser-blow-off plasma are primarily governed by free expansion, while the laser ablated solid target plume conforms to the shock wave model particularly above  $10^{-2}$  mbar. However a bulk Li sample is inevitably more cost effective as it allows for versatility of usage and various theoretical models assist in the analysis of its plume dynamics. A communication to this effect is in preparation.

## 5. Conclusions

Study of plasma plume expansion dynamics of laser ablated lithium solid target in argon, has been carried out with variation in experimental parameters. The plasma emission obtained was observed to comprise excited Li (I) species only; there was no measurable contribution from the background gas. Spectral information derived from measurement of peak intensity and line width, under the assumption of LTE conditions in the plasma, determined the typical plasma characterisation parameters electron temperature ( $T_e$ ) and electron number density ( $n_e$ ). Variation of these parameters in space and time along with evolution of the plasma under different ambient conditions has been investigated. Our results are in accordance with existing theoretical predictions and models put forward to

simulate the interaction and explain consequent complex mechanisms. Evolution of time delay and velocity indicated slowing down of excited Li (I) species beyond 6 mm from the target and for pressures greater than  $10^{-2}$  mbar; a trend which was reflected in the non linear dependence of distance ( $r$ ) on time delay ( $t$ ). Plume expansion dynamics could be adequately described in terms of a shock wave propagation model wherein, the experimental observations made were in excellent agreement with the theoretical predictions.

Temporal dependence of  $T_e$  showed a  $t^{-1}$  variation indicating departure from the theoretical adiabatic expansion model usually applied. It was observed that  $n_e$  varied as  $t^{-2}$  suggesting linear expansion of plasma. In addition,  $n_e$  showed a spatial dependence of  $1/r$  and effectively changed with increase in ambient pressure. The effect of ambient gas was studied and the results analysed in terms of atomic collision processes.

## References

- [1] S S Harilal, P Radhakrishnan, V P N Nampoori and C P G Vallabhan, *Appl. Phys. Lett.* **64**, 3377 (1994)
- [2] D B Geohegan, in *Pulsed laser deposition of thin films* edited by D B Chrisey and G K Hubler (Wiley, New York, 1994)
- [3] M L Brake, J Meachum, R M Gilgenbach and W Thornhill, *IEEE Trans. Plasma Sci.* **PS-15**, 73 (1987)
- [4] J F Ready, in *Effects of high-power laser radiation* (Academic Press, London, 1971)
- [5] H R Griem, in *Plasma spectroscopy* (McGraw Hill, New York, 1964)
- [6] *Plasma Diagnostic Techniques* edited by R H Huddleston and S L Leonard (Academic Press, New York, 1965)
- [7] G Bekefi, *Principles of Laser Plasmas* (Wiley, New York, 1976) p. 549
- [8] H R Griem, *Phys. Rev.* **128**, 515 (1962)
- [9] M A Gigisos, S Mar, C Perez and I de la Rosa, *Phys. Rev.* **E49**, 1575 (1994)
- [10] S S Harilal, C V Bindhu, R C Issac, V P N Nampoori and C P G Vallabhan, *J. Appl. Phys.* **82**, 2140 (1997)
- [11] J Gonzalo, F Vega and C N Afonso, *J. Appl. Phys.* **77**, 6588 (1995)
- [12] I Borthwick, C T J Scott, K W D Ledingham and R Singhal in *Laser Ablation: Mechanisms and Applications-II* edited by J C Miller and D B Geohegan (AIP 288, NY, 1994) p. 414
- [13] C Germain, C Girault, R Gisbert, J Aubreton and A Catherinot, in *Laser ablation: Mechanisms and applications-II* edited by J C Miller and D B Geohegan (AIP 288, NY, 1994) p. 183
- [14] R K Singh, O W Holland and J Narayan, *J. Appl. Phys.* **68**, 233 (1990)
- [15] D B Geohegan, *Appl. Phys. Lett.* **60**, 2732 (1992)
- [16] Y B Zel'dovich and Y P Raizer, in *Physics of shock waves and high temperature hydrodynamic phenomena* (Academic Press, New York, 1967) vol. I
- [17] P T Rumsby and J W M Paul, *Plasma Phys.* **16**, 247 (1974)
- [18] R Tambay, R Singh and R K Thareja, *J. Appl. Phys.* **72**, 1197 (1992)
- [19] N Singh, M Razafinimanana and A Gleizes, *J. Phys.* **D31**, 2921 (1998)